SUPPORTING INFORMATION

Variable Doping Induces Mechanism Swapping in Electrogenerated Chemiluminescence of $Ru(bpy)_3^{2+}$ Core-shell Silica Nanoparticles.

Giovanni Valenti,[1‡] Enrico Rampazzo,[1‡] Sara Bonacchi,[1,†] Luca Petrizza,[1] Massimo Marcaccio,[1] Marco Montalti,[1] Luca Prodi,[1] Francesco Paolucci[1,2*].*

[1]Department of Chemistry ''Giacomo Ciamician'', University of Bologna, Via Selmi 2, 40126 Bologna, Italy.

[2] ICMATE-CNR Bologna Associate Unit, University of Bologna, via Selmi 2, 40126, Bologna, Italy.

* L.Pr. luca.prodi@unibo.it; F.P. francesco.paolucci@unibo.it

Table of contents

1) Trasmission Electron Microscopy (TEM) analysis

TEM images of NPs samples were obtained with a Philips CM 100 microscope, operating at 80 kV, and using 3.05 mm copper grids (Formvar support film - 400 mesh). A drop of NIR-PluS NPs solution diluted with water (1:50) was placed on the grid and then dried under vacuum. The TEM images showing the denser silica cores, were analyzed with the ImageJ software. Histogram were fitted according to a Gaussian distribution obtaining the average diameter ± SD for the silica nanoparticles core.

Table S1: NIR-PluS NPs silica core mean diameter ± SD determined by TEM analysis.

Sample	*(d_{core} ± SD) [nm]*
Ru@NP1	10.2 ± 1.4
Ru@NP2	10 ± 2
Ru@NP3	11 ± 3
Ru@NP4	9 ± 2
Ru@NP5	9 ± 2
Ru@NP6	9.6 ± 2.4

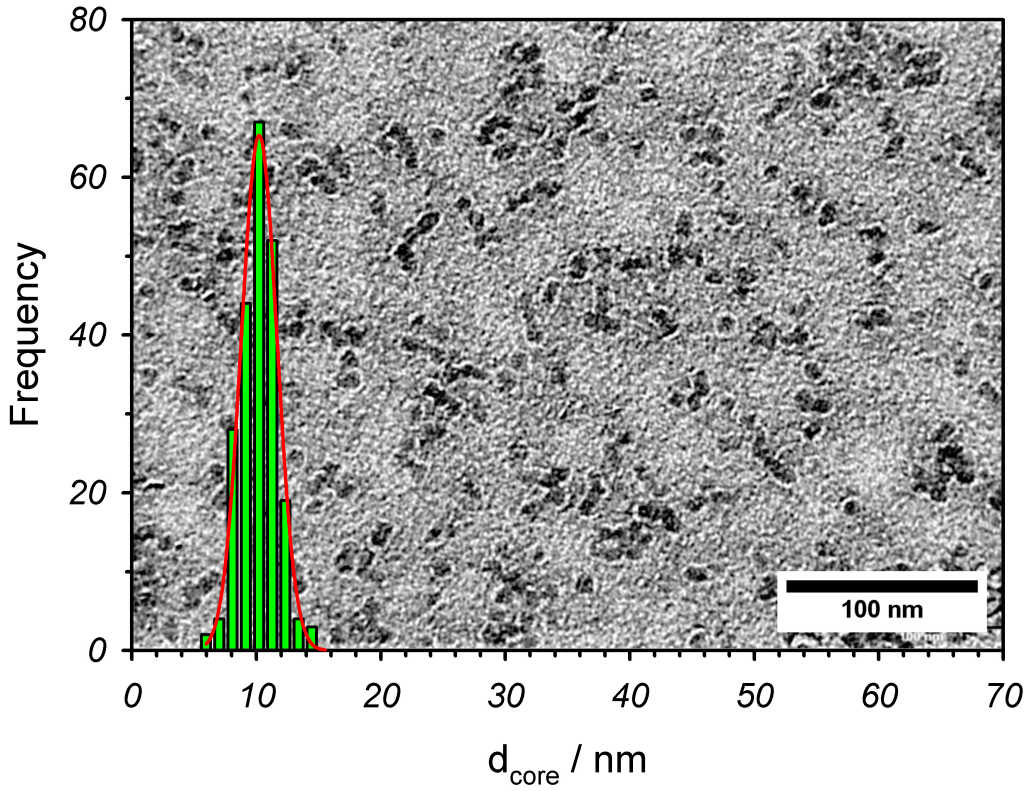

Figure S1: **Ru@NP1**, TEM image and silica core size distribution: d = (10.2 ± 1.4) nm.

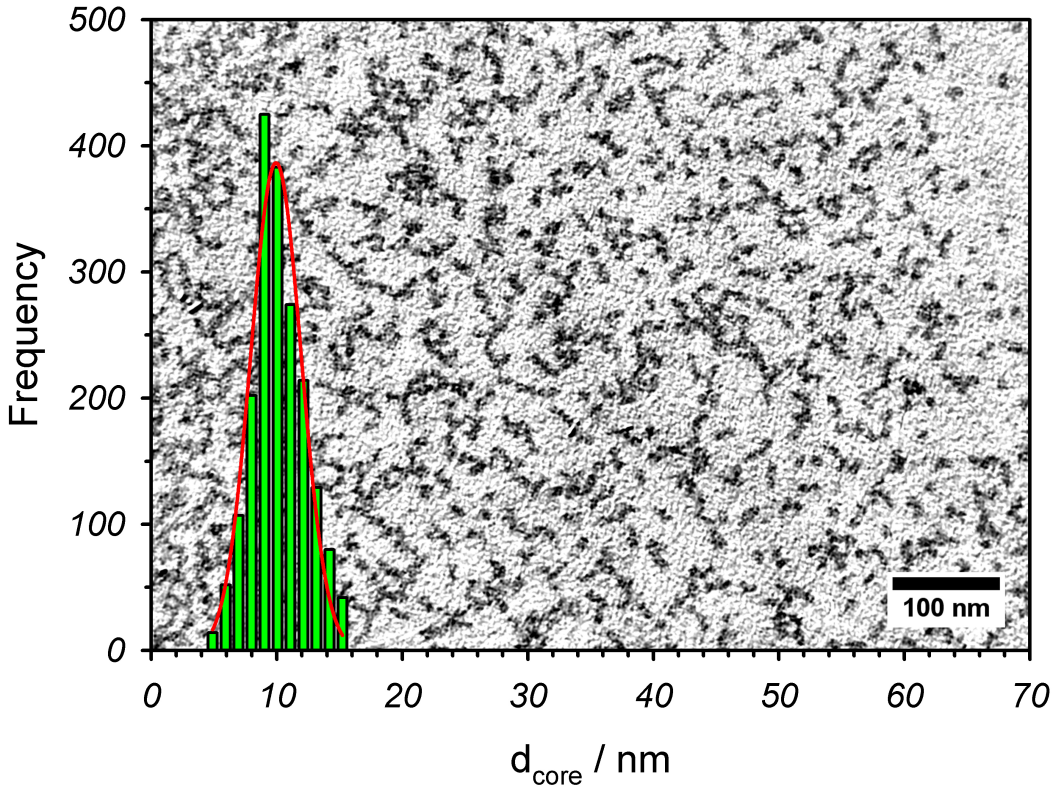

Figure S2: **Ru@NP2**, TEM image and silica core size distribution: d = (10 ± 2) nm.

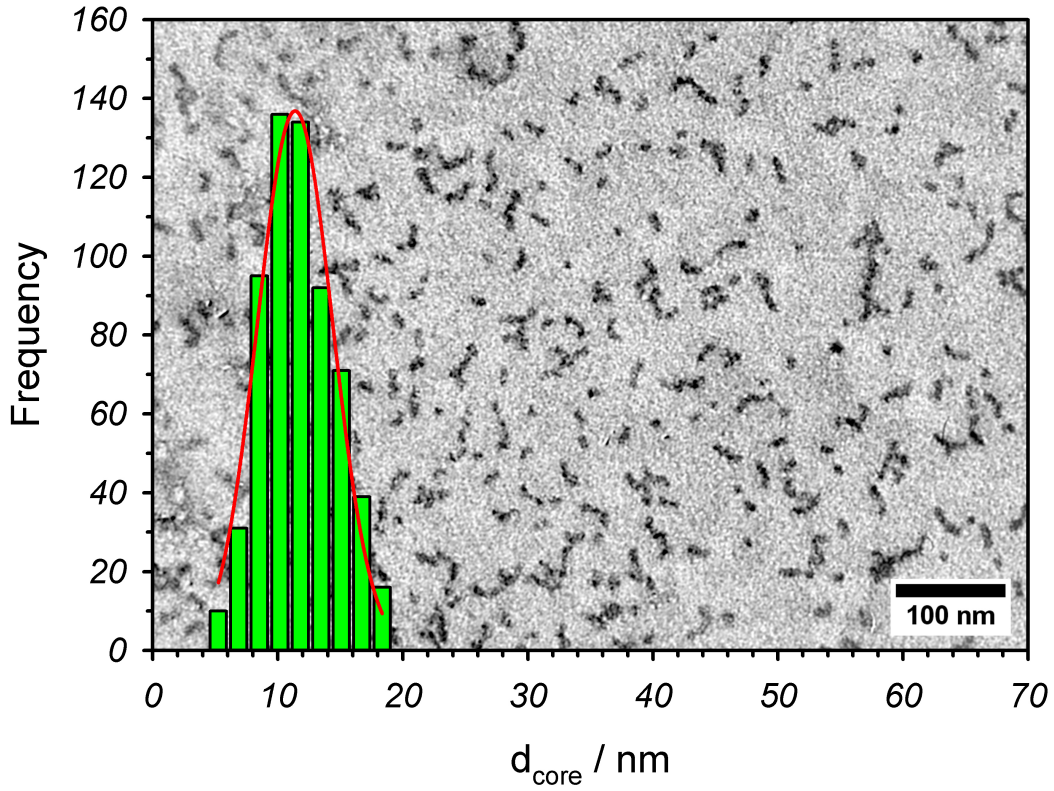

Figure S3: **Ru@NP3**, TEM image and silica core size distribution: d = (11 ± 3) nm.

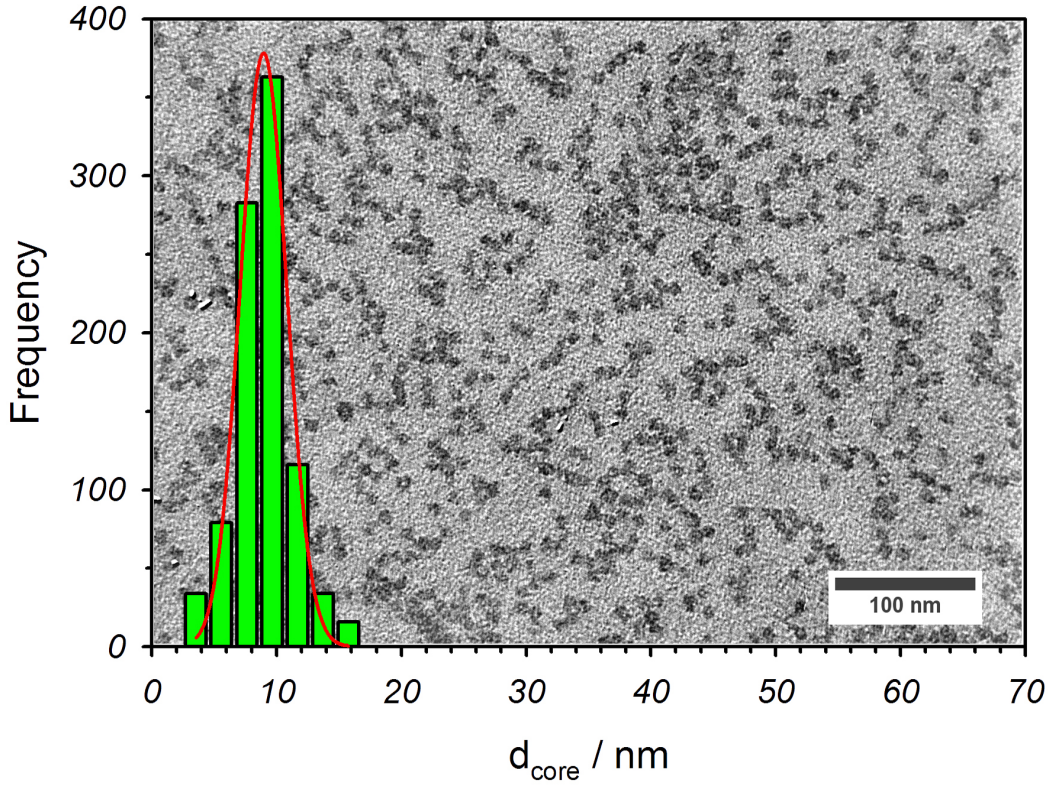

Figure S4: **Ru@NP4**, TEM image and silica core size distribution: d = (9 ± 2) nm.

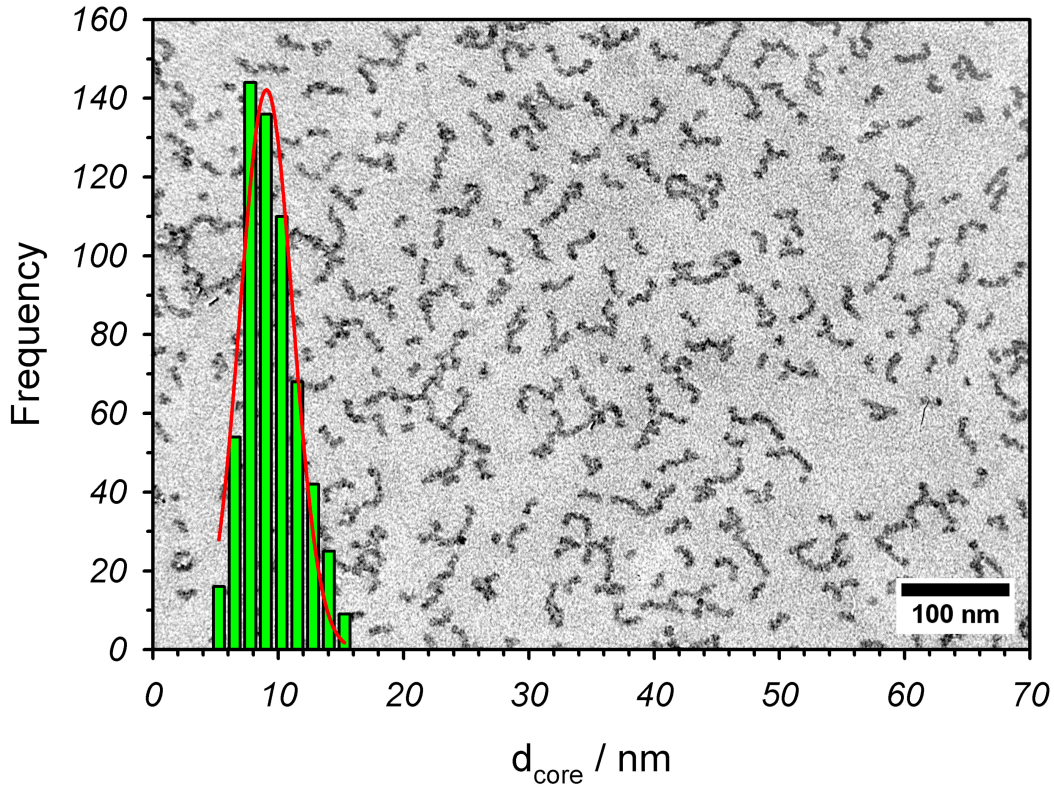

Figure S5: **Ru@NP5**, TEM image and silica core size distribution: d = (9 ± 2) nm.

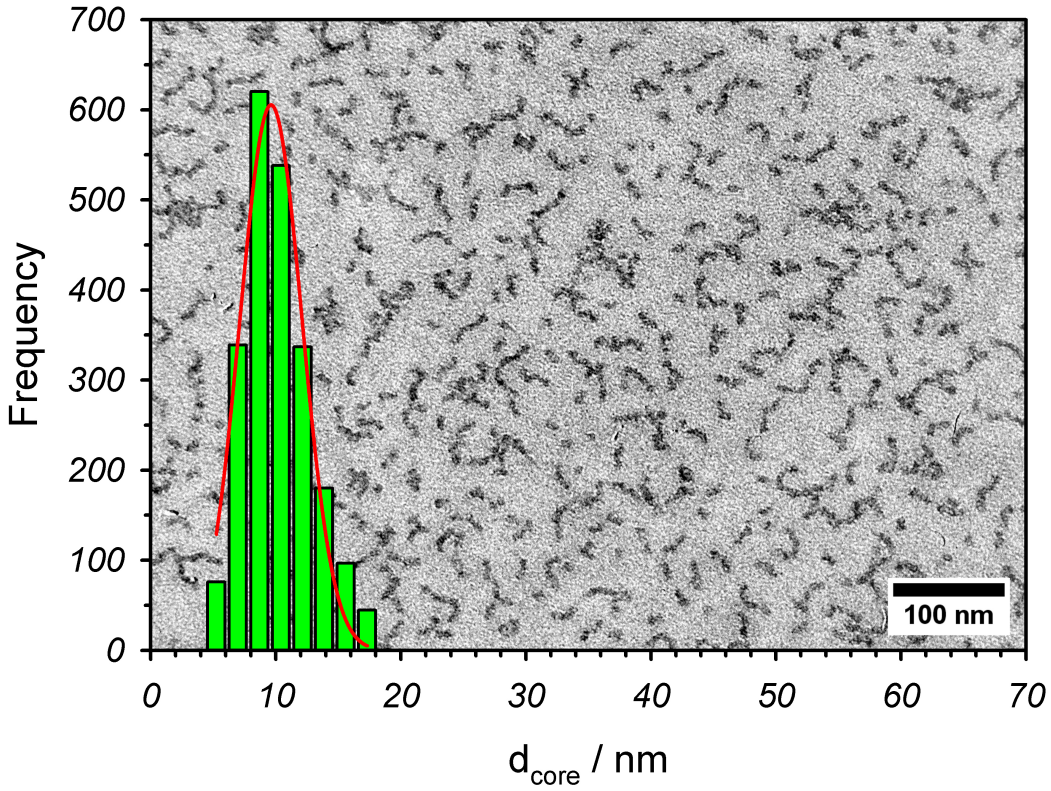

Figure S6: **Ru@NP6**, TEM image and silica core size distribution: d = (9.6 ± 2.4) nm.

2) Dynamic Light Scattering (DLS) analysis

NPs hydrodynamic diameter (d_H) distributions were obtained in water at 25°C through DLS measurements (Malvern Nano ZS instrument, 633 nm laser diode). Samples were filtered with 0.22 µm RC filters and then housed in disposable polystyrene cuvettes of 1 cm optical path length, using water as solvent. The average width of DLS hydrodynamic diameter distribution is indicated by PdI (Polydispersion Index). In case of a mono-modal distribution (gaussian) calculated by means of cumulant analysis, $PdI=(\sigma/Z_{avg})^2$, where σ is the width of the distribution and Z_{avg} is average diameter of the particles population respectively. Standard deviation (SD) is calculatate over five different measurements.

As shown by the TEM images, all the NIR-PluS NPs had very similar average silica core diameters. In some cases the average hydrodynamic diameter measured by DLS analysis was slightly higher than the expected average value (25-30 nm). The DLS technique over-weight the average size for a colloidal sample with moderate polydispersity (PdI = 0.2): for this reason the size distribution by number are showed to represent a more realistic picture of the hydrodynamic diameter of NPs in sospension.

Table S2: DLS Hydrodynamic diameter values in water for the nanoparticles samples described in this work. Standard deviation was calculated on five different measurements.

Sample	d_H ± SD [nm]	PdI
Ru@NP1	19 ± 3	0.30
Ru@NP2	18 ± 5	0.24
Ru@NP3	27 ± 5	0.22
Ru@NP4	22 ± 3	0.15
Ru@NP5	35 ± 5	0.13
Ru@NP6	32 ± 6	0.17

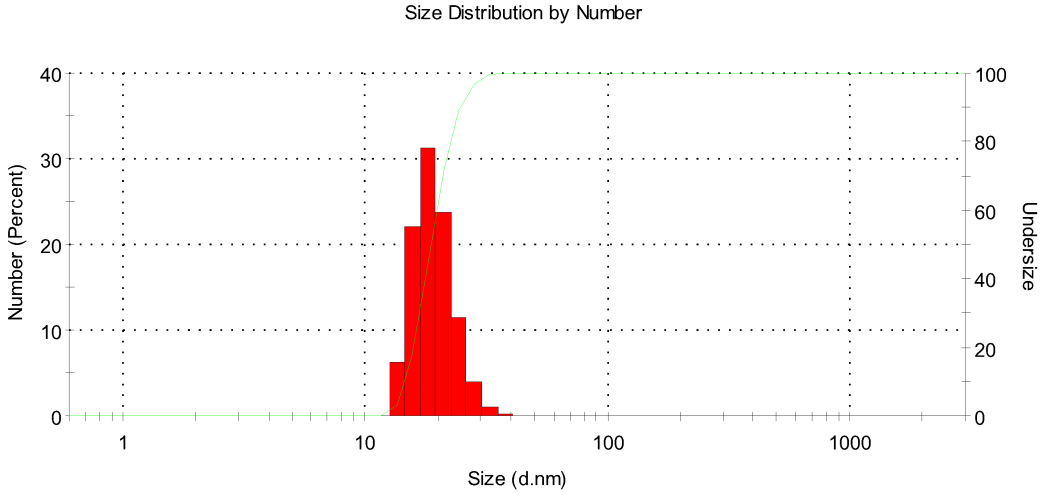

Figure S7: DLS diameter distribution by number of **Ru@NP1** (d_H = 19 ± 3 nm; water, 25°C).

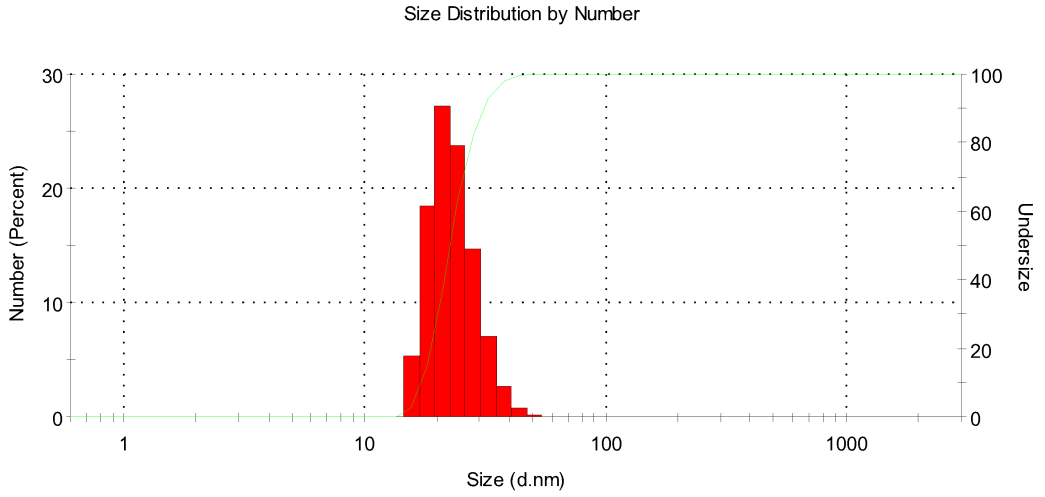

Figure S8: DLS diameter distribution by number of **Ru@NP2** (d_H = 18 ± 5 nm; water, 25°C).

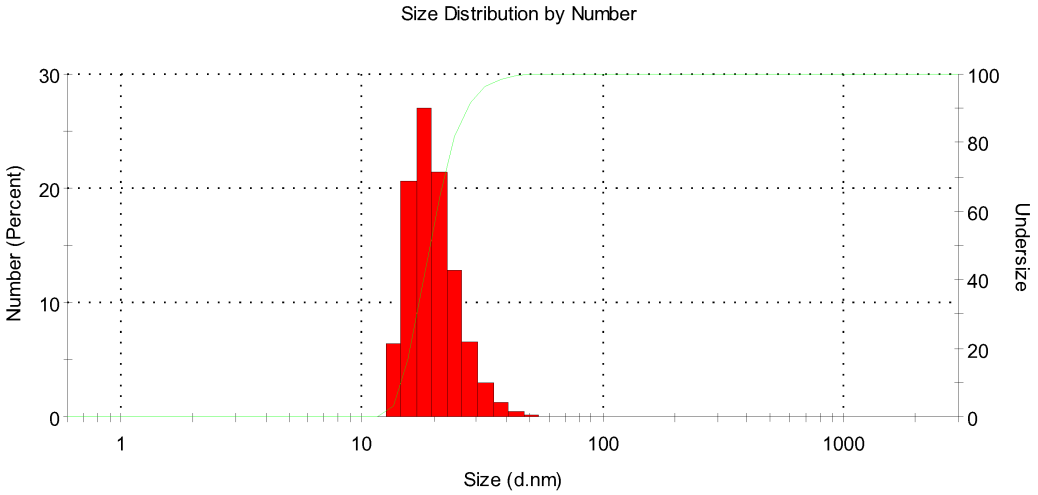

Figure S9: DLS diameter distribution by number of **Ru@NP3** (d_H = 27 ± 5 nm; water, 25°C).

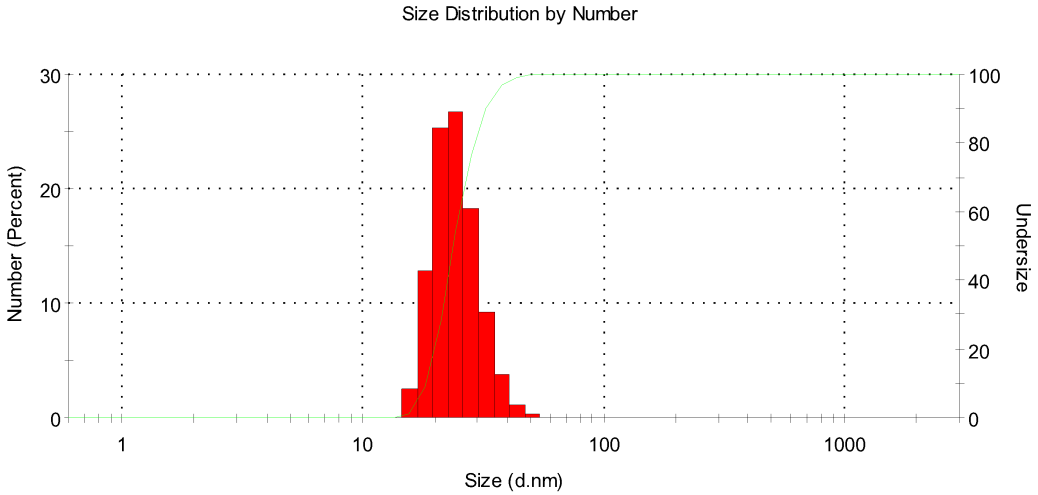

Figure S10: DLS diameter distribution by number of **Ru@NP4** (d_H = 22 ± 3 nm; water, 25°C).

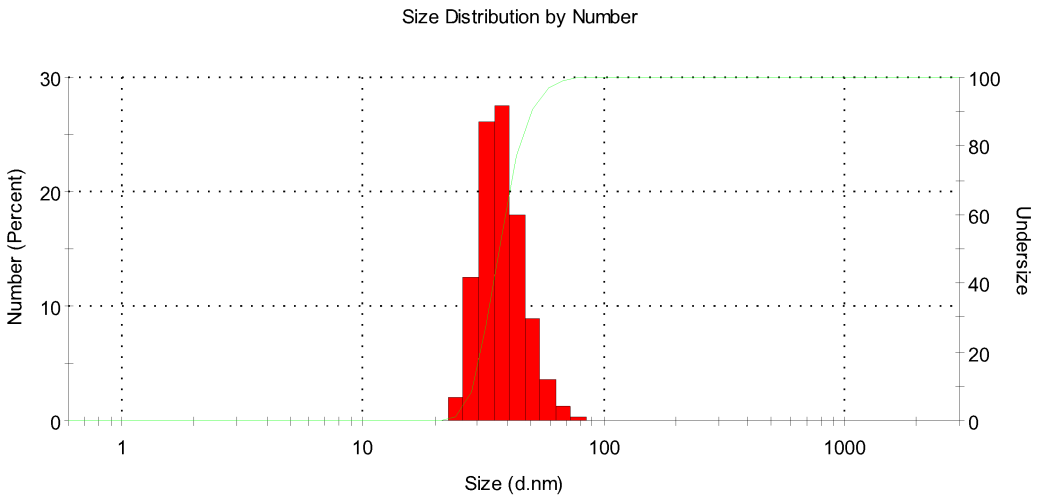

Figure S11: DLS diameter distribution by number of **Ru@NP5** (d_H = 35 ± 5 nm; water, 25°C).

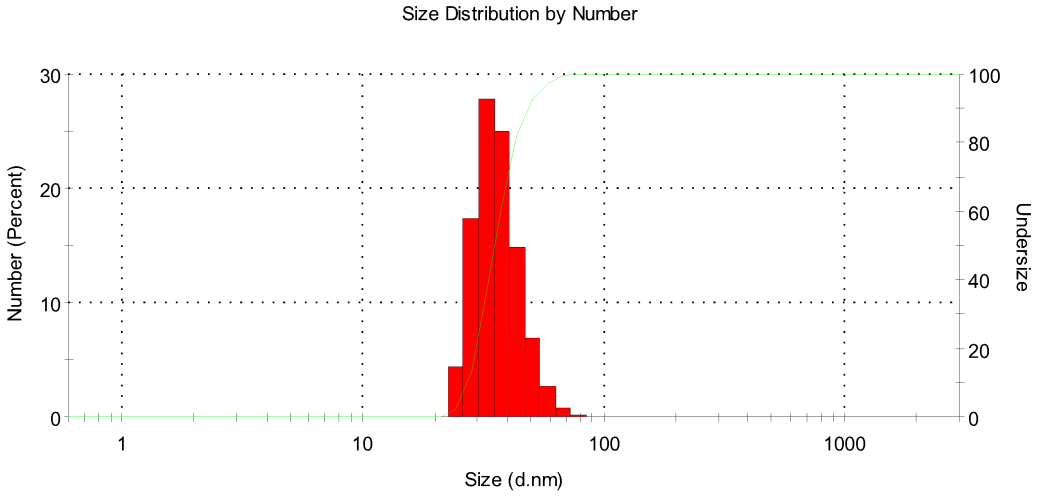

Figure S12: DLS diameter distribution by number of **Ru@NP6** (d_H = 32 ± 6 nm; water, 25°C).

2) ζ-Potential analysis

NPs ζ-Potenzial values were obtained using a Malvern Nano ZS instrument equipped with a 633 nm laser diode. Samples were housed in disposable polycarbonate folded capillary cell (DTS1070, 750 µL, 4 mm optical path length). Electrophoretic determination of ζ-Potential was made using a auto-mode setup (Smoluchowski approximation) in acqueous media (conditions : [**Ru@NP**] = 4 µM, [KCl] = 1 mM; [phosphate buffer] = 1 mM, pH 7.0, T = 25 °C, samples filtered with a 200 nm RC syringe filter).

Table S3: ζ-Potential values in water for the nanoparticles samples described in this work. Standard deviation was calculated over ten different measurements.

Sample	***ζ-Potential ± SD (mV)***
Ru@NP1	-10.0 ± 1.5
Ru@NP2	-6.3 ± 0.9
Ru@NP3	-4.4 ± 1.0
Ru@NP4	-2.5 ± 1.2
Ru@NP5	-0.9 ± 0.7
Ru@NP6	0.9 ± 0.8

3) Absorption spectra

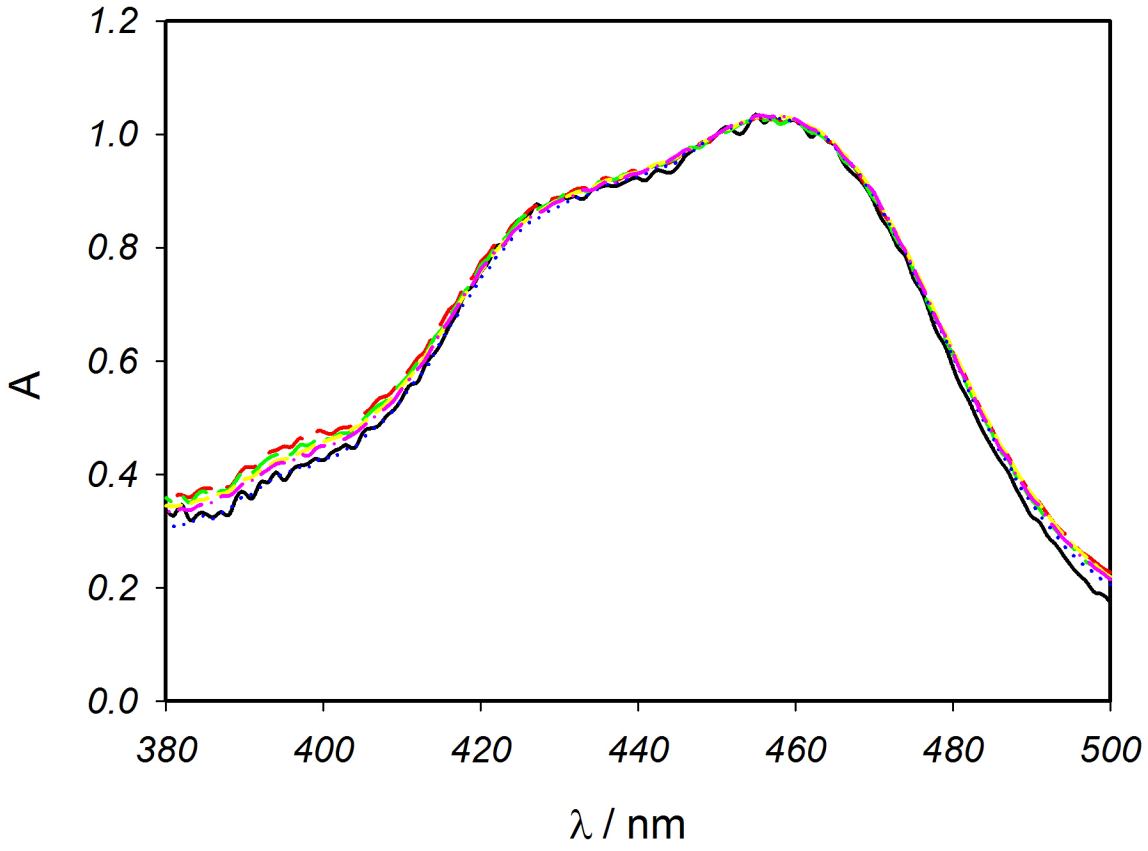

Figure S13: Normalized absorption spectra of samples **Ru@NP1-6**. Conditions: water, [**Ru@NP**] = 10 µM filtered with a RC 200 µm filter.

4) Electrochemiluminescence

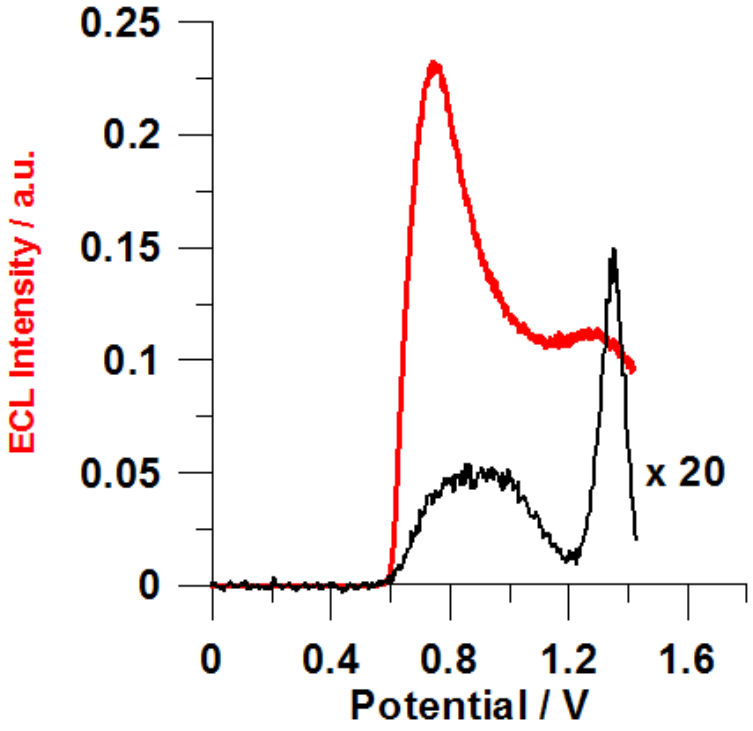

Figure S14. ECL intensity vs potential curves of **Ru@NP1** (Ru/NP = 2) in 100 mM PB solutions with 30 mM DBAE (red curve) or with 30 mM tripropylamine (black curve) as co-reactant; scan rate 0.1 V s^{-1}(E vs. SCE); PMT bias 750 V.

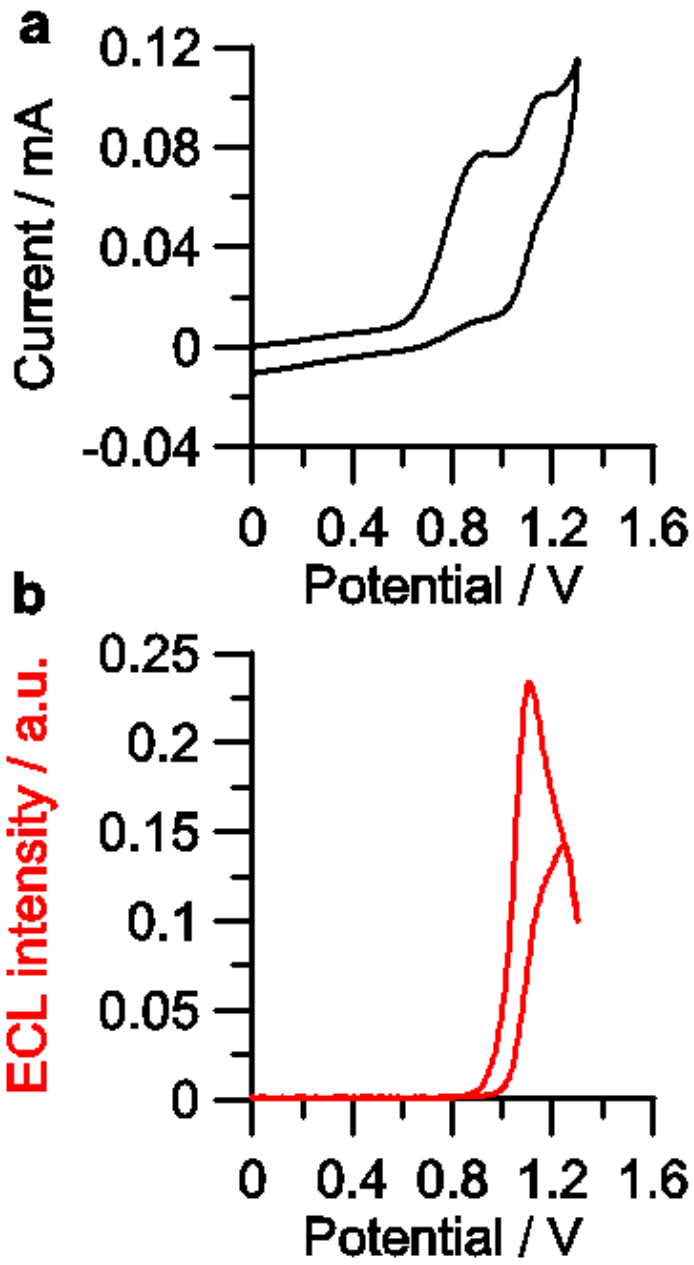

Figure S15 Cyclic voltammetry (a) and ECL intensity (b) vs potential curves of $Ru(bpy)_3^{2+}$ 320 μM in 100 mM PB solutions, 30 mM DBAE as coreactant; scan rate 0.1 V s^{-1}(E vs. SCE); PMT bias 750 V.

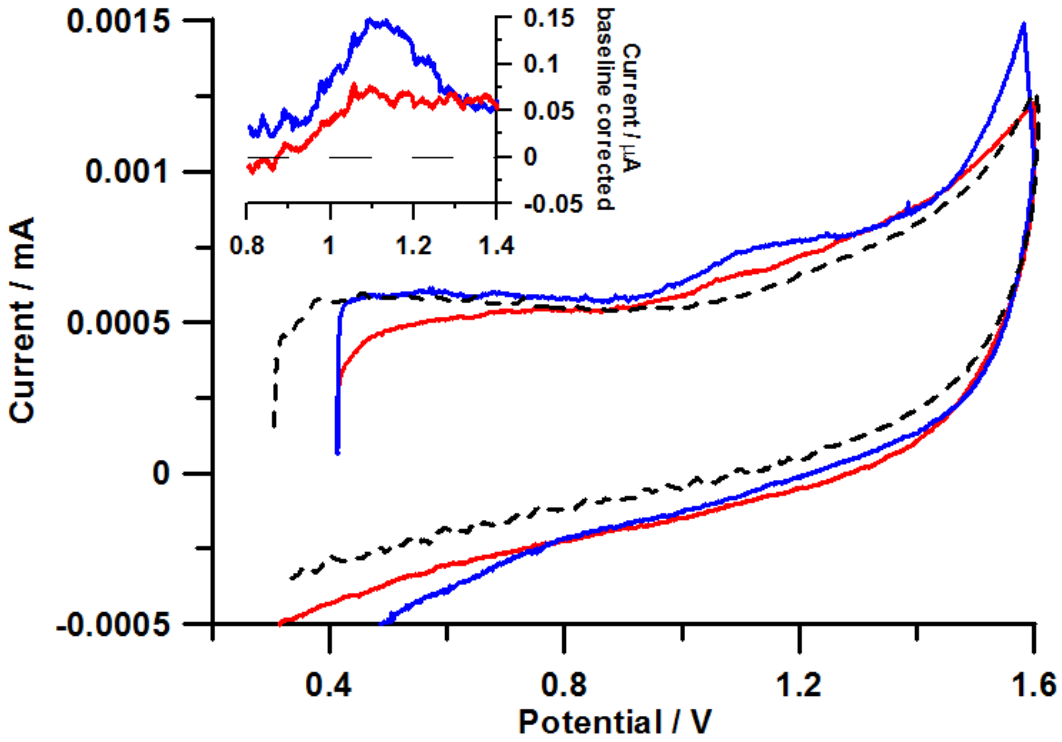

Figure S16 Cyclic voltammetry of DDSNs with different doping (**Ru@NP3** red curve and **Ru@NP6** blue curve) and the pristine (ITO) electrode (black dashed curve). The DDSN samples were prepared on the substrate working electrode (ITO) by deposition of 10 µl of the respective DDSN solution (water 80 µM). Those were then allowed to dry in the dark for at least 12 h and investigated by cyclic voltammetry in CH_3CN 0.05 M Bu_4NPF_6. In the inset is reported the cyclic voltammetry corrected for the baseline of the pristine ITO electrode (dashed line in the main panel). Scan rate 10 mV s^{-1}(E vs. SCE).

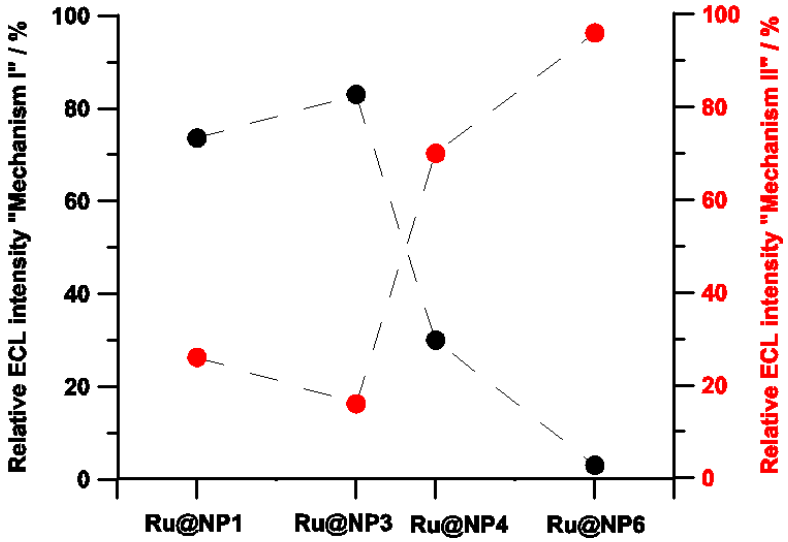

Figure S17 Relative ECL intensity for DDSNs with different doping (2, 6, 16, 24). The intensities were obtained from figure 8 by integrating the ECL intensity related to the first (black dots) or to the second (red dots) ECL peak and normalize for the whole ECL emission. Conditions: 100 mM PB solutions, 30 mM DBAE as coreactant; applied potential 1.4 V for 0.5 sec. (E vs. SCE); PMT bias 750 V.

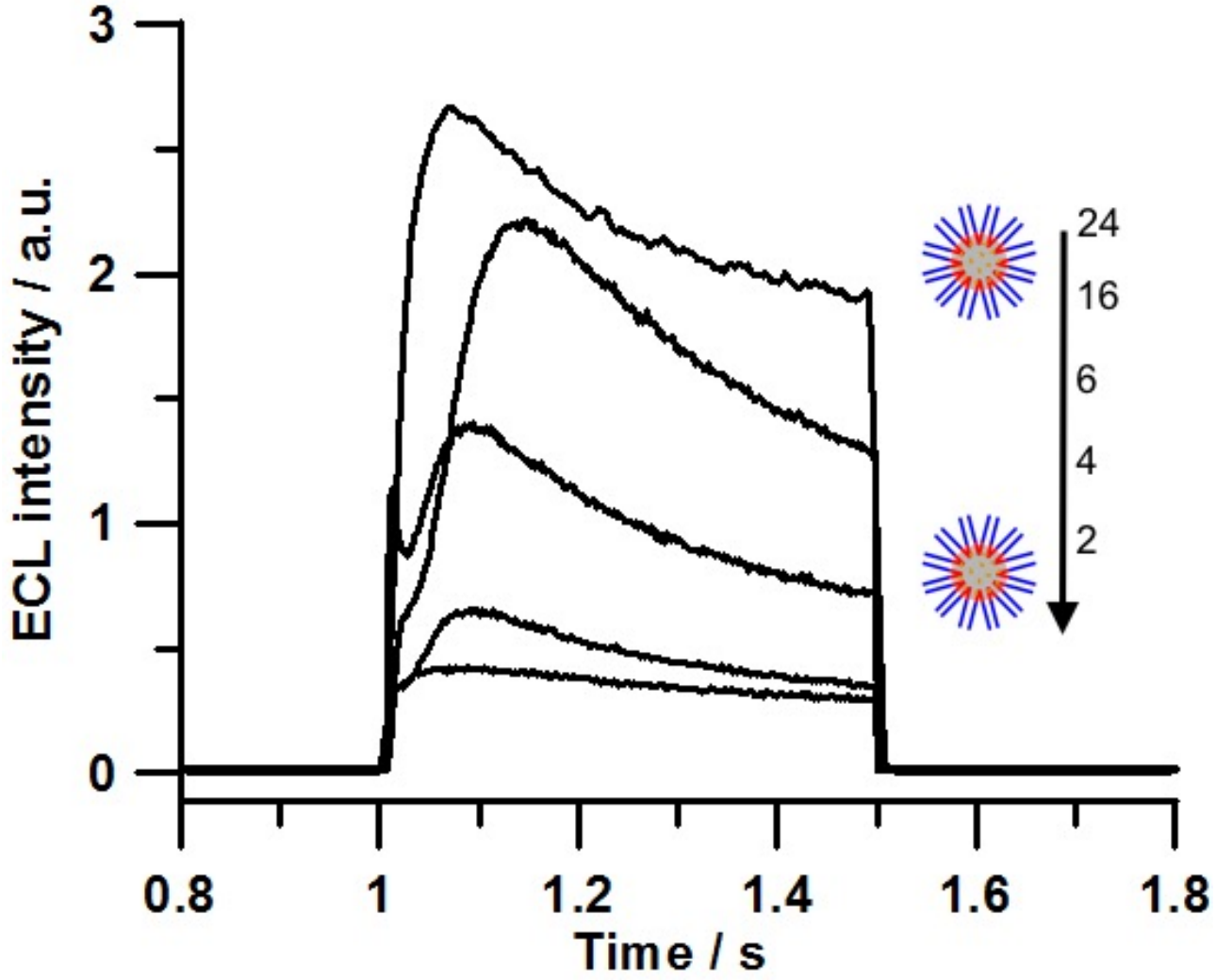

Figure S18 ECL emission vs time of DDSNs with different doping (2, 4, 6, 20, 24). Conditions: 100 mM PB solutions, 30 mM DBAE as coreactant; applied potential 1.4 V for 0.5 sec. (E vs. SCE); PMT bias 750 V.